Competition Between the Pseudogap and Superconducting States of Bi_{2}Sr_{2}Ca_{0.92}Y_{0.08}Cu_{2}O_{8+δ} Single Crystals Revealed by Ultrafast Broadband Optical Reflectivity

G. Coslovich, C. Giannetti, F. Cilento, S. Dal Conte, T. Abebaw, D. Bossini, G. Ferrini, H. Eisaki, M. Greven, A. Damascelli, and F. Parmigiani

Phys. Rev. Lett. **110**, 107003 — Published 6 March 2013

DOI: 10.1103/PhysRevLett.110.107003

Competition between the Pseudogap and Superconducting States of $Bi_2Sr_2Ca_{0.92}Y_{0.08}Cu_2O_{8+\delta}$ Single Crystals Revealed by Ultrafast Broadband Optical Reflectivity

G. Coslovich,[1,*] C. Giannetti,[2,3] F. Cilento,[1,4] S. Dal Conte,[2,3] T. Abebaw,[1,†] D. Bossini,[3,‡] G. Ferrini,[2,3] H. Eisaki,[5] M. Greven,[6] A. Damascelli,[7,8] and F. Parmigiani[1,4]

[1] *Department of Physics, Università degli Studi di Trieste, Trieste I-34127, Italy*
[2] *I-LAMP (Interdisciplinary Laboratories for Advanced Materials Physics), Università Cattolica del Sacro Cuore, Brescia I-25121, Italy.*
[3] *Department of Physics, Università Cattolica del Sacro Cuore, Brescia I-25121, Italy*
[4] *Sincrotrone Trieste S.C.p.A., Basovizza I-34012, Italy*
[5] *Nanoelectronics Research Institute, National Institute of Advanced Industrial Science and Technology, Tsukuba, Ibaraki 305-8568, Japan*
[6] *School of Physics and Astronomy, University of Minnesota, Minneapolis, Minnesota 55455, USA*
[7] *Department of Physics & Astronomy, University of British Columbia, Vancouver, British Columbia V6T 1Z1, Canada*
[8] *Quantum Matter Institute, University of British Columbia, Vancouver, British Columbia V6T 1Z4, Canada*

Ultrafast broadband transient reflectivity experiments are performed to study the interplay between the non-equilibrium dynamics of the pseudogap and the superconducting phases in $Bi_2Sr_2Ca_{0.92}Y_{0.08}Cu_2O_{8+\delta}$. Once superconductivity is established the relaxation of the pseudogap proceeds ~ 2 times faster than in the normal state, and the corresponding transient reflectivity variation changes sign after ~ 0.5 ps. The results can be described by a set of coupled differential equations for the pseudogap and for the superconducting order parameter. The sign and strength of the coupling term suggest a remarkably weak competition between the two phases, allowing their coexistence.

PACS numbers: 74.40.Gh, 74.25.nd, 74.72.Kf, 78.47.jg

In cuprates [1], pnictides [2], manganites [3] and heavy-fermion compounds [4] low-energy gaps follow the formation of multiple ordered phases, generally interacting with each other. Their mutual coupling, i.e., the mixed terms in a multi-component Ginzburg-Landau (GL) free energy expansion, plays a key role in determining the unconventional electronic properties of these materials [5–8]. A particularly interesting case is given by the pseudogap (PG) and superconducting (SC) phases in cuprates, where the debate between a competing order (positive free energy coupling term) [9, 10] or a cooperative order scenario (negative free energy coupling term)[11, 12] is still unresolved.

So far this problem has been approached by measuring the excitation spectra and low-energy gaps of each phase in equilibrium conditions throughout the phase diagram. Angle-resolved photoemission spectroscopy and scanning tunneling spectroscopy have successfully distinguished almost degenerate low-energy gaps in cuprates [13, 14]. However, at equilibrium the coupling between coexisting phases can hardly be observed for the free energy is kept at minimum and the different contributions cannot be disentangled. Conversely, ultrafast time-resolved spectroscopy can address this fundamental issue by investigating the non-equilibrium dynamics of the interacting phases after a sudden non-thermal photoexcitation [15, 16]. Above all, the possibility to create a transient non-thermal phase, where only one of the order parameters is selectively quenched, is critical for directly measuring the coupling between order parameters. In particular, in the limit of the *local equilibrium approximation* [17], and for excitation densities well below saturation [18], the non-equilibrium dynamics of the order parameter and its corresponding excitations coincide [19]. Thus the dynamics of the order parameters can be probed in real-time by measuring the reflectivity variation, $\Delta R/R$. Furthermore, a broad spectral range of probing photon energies is needed to disentangle the dynamics of different interacting order parameters [16].

In this Letter, ultrafast broadband transient reflectivity experiments allow to identify and observe the dynamics of PG and SC phases in underdoped $Bi_2Sr_2Ca_{0.92}Y_{0.08}Cu_2O_{8+\delta}$ single crystals (T_C = 85 K). Singular Value Decomposition (SVD) is applied to disentangle their spectro-temporal fingerprints in the out-of-equilibrium reflectivity data. At low pump fluence (10 μJ/cm^2) the recovery dynamics of the PG proceeds ~ 2 times faster once the SC order parameter is established, and eventually the corresponding transient reflectivity variation changes sign after ~ 0.5 ps. Furthermore, the amplitude of the PG perturbation decreases by a factor 2 below T_C. These results prove the existence of a coupled dynamics for the PG and for the SC order parameter, which can be described by a set of differential equations with a coupling term connecting their relaxation dynamics. Under the assumption that the PG phase has a broken symmetry, the time-dependent GL approach provides a framework for interpreting the coupling term as a positive interaction between order parameters in the GL expansion of the free energy. Quantitive estimations suggest that the interaction is weak enough for allowing the coexistence of the two competing phases. This experiment represents a benchmark for the recent developments of theoretical non-equilibrium methods beyond quasi-equilibrium approximations, where the interplay between superconductivity and pseudogap might arise at the quantum level [20].

The dynamics of the non-equilibrium optical response is probed by combining the supercontinuum light generation and detection in the 1.1-2 eV spectral region using a photonic crystal fiber (set-up described in [21]) and an Optical Parametric Amplifier (OPA) with output in the 0.5-1.1 eV range [22]. The experiments are performed on high quality underdoped $Bi_2Sr_2Ca_{0.92}Y_{0.08}Cu_2O_{8+\delta}$ single crystals (T_c = 85 K). The sample growth and annealing methods are the same as previously reported [23, 24].

Figs. 1a and 1b show the transient perturbations of the reflectivity as a function of both time delay and probe photon energy as measured for the PG and SC phases respectively. The experiment is performed at low fluence (10 μJ/cm^2), where the ΔR/R signal is roughly proportional to the perturbation of the order parameters [17–19]. The 2D matrices, ΔR/R(E,t), have been decomposed through SVD, i.e., by calculating the corresponding l-rank matrix, $\sum_{k=1}^{l}\Delta\phi_k(\mathrm{E})\Delta\psi_k(\mathrm{t})$, that best reproduces the experimental data, where $\Delta\psi_k$(t) is the temporal eigenfunction normalized to its maximum and $\Delta\phi_k$(E) is the spectral eigenfunction, containing information about the absolute magnitude of the peak signal at each energy E [22]. This method, which has been widely applied in several research areas [25, 26], yields both energy- and time-domain information, and allows the identification of a minimal number of spectro-temporal components that reproduce a set of data [26]. These components are sorted considering their relative weight, with the first component generally accounting for $\sim$ 80% of the signal and the second for $\sim$ 10 %. Higher order components generally represent the experimental noise. In fact, the first component alone gives a fair and almost noise-free representation of the experimental data (see insets of Fig. 1c and 1d).

The spectral eigenfunction of the first component obtained in the PG phase (T = 100 K) is peaked at about 1.2 eV and becomes negative at photon energies higher than 1.4 eV (Fig. 1c). The second component obtained in the PG phase is the remnant normal state signal observed at room temperature [27] and is not relevant in this work. Below T_C the energy-time response changes dramatically with the appearance of a new first component, exhibiting a large positive plateau above 1.2 eV and a sign change below 1.1 eV (Fig. 1d, T = 20 K). This first component originates from photoexcitations across the SC gap causing the transfer of spectral weight in the interband spectral region [24].

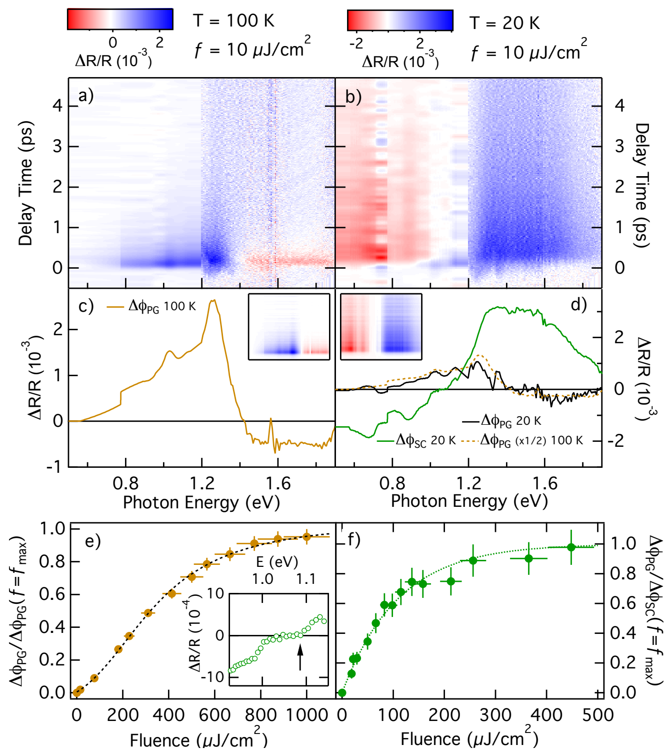

FIG. 1. Time-energy matrices of reflectivity variations at 100 K (a) and 20 K (b) at low fluence (10 μJ/cm^2) on underdoped $Bi_2Sr_2Ca_{0.92}Y_{0.08}Cu_2O_{8+\delta}$. The data are shown in false color scale. c), d) Spectral traces of the SVD components at 100 K and 20 K respectively. The insets show the spectra-temporal matrix of the component with the same scale used in a) and b). e), f) Fluence dependence of the PG and SC components respectively, measured at fixed probe energies (see text). Each experimental point is normalized to the high fluence limit. The dotted lines are fits with a non-linear function [22] exhibiting exponential suppression at low-fluence (e) and saturation at high fluence (e and f) of the form $\propto 1 - e^{-f/f_{sat}}$, with $f_{sat}^{PG} \sim 400$ μJ/cm^2 and $f_{sat}^{SC} \sim 100$ μJ/cm^2. The SC component around 1.1 eV is shown in the inset of (e).

In the SC phase the second component of the SVD becomes significant. Remarkably this component exhibits the same spectral shape of the PG signal at 100 K, but with half the amplitude at the same pump fluence (Fig. 1d). Further details can be obtained by considering the probe photon energy where the SC component has a node (1.08 eV, see inset of Fig. 1e), and hence the $\Delta R/R$ signal is dominated by the PG signal. The fluence dependence at this probe photon energy (Fig. 1e) exhibits a saturation threshold ($f_{sat} \sim 400$ μJ/cm^2) similar to the one measured at 100 K, and clearly different from the saturation fluence observed at 0.5 eV ($\sim$ 100 μJ/cm^2, see Fig. 1f), where instead the SC component is maximal.

These results are consistent with a scenario where the PG and SC phases coexist below T_C and compete in the absorption of the pump photon energy. In previous time-resolved single-color experiments at 800 nm (1.5 eV) the

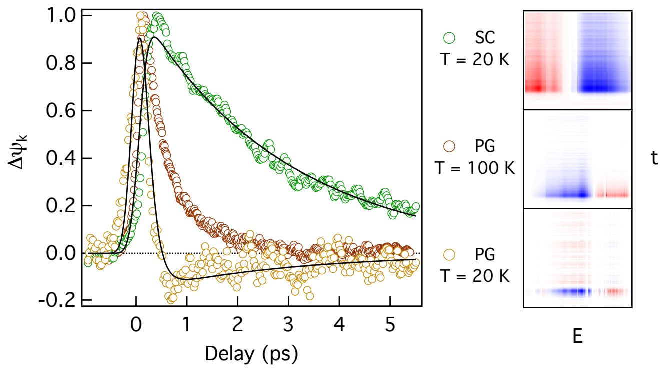

FIG. 2. Temporal traces, $\Delta\psi_k(t)$, of the first two SVD components obtained at T = 20 K, (data of Fig. 1) and the fit obtained by the set of coupled differential equations, Eq. 1. The PG component at 100 K is shown for comparison. As a reference, the insets on the right side show the spectro-temporal matrices of each components with the same scale used in Fig. 1a and 1b.

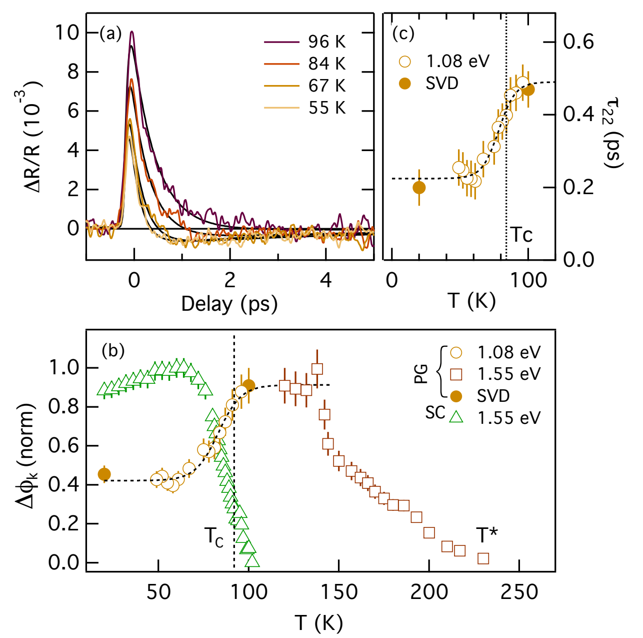

FIG. 3. a) Transient reflectivity variation of the PG component measured at 1.08 eV photon energy and pump fluence of $\sim$ 50 μJ/cm^2 as a function of temperature. Black solid lines are fits to Eq. (1). b) Temperature dependence of SC and PG components normalized to the maximal value in the 20-250 K temperature range. c) Temperature dependence of the initial decay time of the PG component. Empty circles, squares and triangles are data taken at a single photon energy, full circles are obtained through SVD analysis of the full spectrum. To improve the signal-to-noise ratio in this low-fluence measurements the PG component is measured at 1.08 eV below T_C and at 1.55 eV above. For the same reason the SC component is measured at 1.55 eV instead of 0.5 eV, as the PG signal remains negligible also at this photon energy in the low-fluence limit. Dashed lines are guides to the eye.

residual PG phase component below T$_C$ was hidden by the large SC phase response [18]. These results, while confirming previous experiments reporting the coexistence of two dynamics below T$_C$ [16], allow for the first time the unambiguous and precise measurement of both ψ_k(t) dynamics by recognizing their spectro-temporal fingerprints with no *a priori* assumptions.

The results concerning the non-equilibrium dynamics of PG and SC components are shown in Fig. 2. The PG recovery dynamics drastically changes below T$_C$ exhibiting a $\sim$ 2 times faster initial decay time and a change of sign after $\sim$ 500 fs. Because of this sign change, such dynamics cannot represent a simple quasiparticle density relaxation process. The dynamics of both components can be reproduced by a set of coupled differential equations of the form:

$$\frac{d}{dt}\begin{pmatrix}\Delta\psi_{SC}\\ \Delta\psi_{PG}\end{pmatrix} = \begin{pmatrix}I_{SC}(t)\\ I_{PG}(t)\end{pmatrix} - \begin{pmatrix}\tau_{11}^{-1} & \tau_{12}^{-1}\\ \tau_{21}^{-1} & \tau_{22}^{-1}\end{pmatrix}\begin{pmatrix}\Delta\psi_{SC}\\ \Delta\psi_{PG}\end{pmatrix} \quad (1)$$

where $I_{SC}(t)$ and $I_{PG}(t)$ are the external perturbations induced by the pump pulse, and τ_{11}, τ_{22}, τ_{12}, τ_{21}, represent the diagonal and mixed relaxation terms for the SC (1) and the PG (2) components. The amplitude of the initial perturbations $\Delta\psi_k(t=0)$ can be fixed by considering that the condition of $\Delta\psi_k(t=0)$=1 is reached at the saturation in the high fluence limit (Fig. 1e and Fig.1f), i.e., when the photo-induced vaporization of the ordered phase occurs [18]. The non-equilibrium dynamics of both SC and PG can be simultaneously reproduced by Eq. 1 (Fig. 2). The τ_{22} value obtained at 20 K is substantially lower than τ_{22} at 100 K data (decreasing from about $\sim$ 0.5 ps to $\sim$ 0.2 ps) and a non-zero mixed term, $\tau_{21} \sim 17$ ps, is found. On the other hand τ_{12} has a negligible effect on the dynamics since the PG component is perturbed one order of magnitude less than the SC component.

The detailed temperature dependence of the PG component dynamics can be measured at 1.08 eV (Fig. 3), where the highest contrast is obtained over the SC component, as previously discussed. The absence of a long decay signal (for $t > 5$ ps) further confirms that the SC component remains negligible up to T$_C$. The initial relative perturbation of both PG and SC components is shown in Fig.3b as a function of temperature. The trend of the perturbation amplitude of the SC phase is related to the temperature dependence of the equilibrium SC order parameter [18]. Instead the suppression of the PG is inversely proportional to the SC order parameter, with a sharp transition at T_C. A similar transition can be observed in the initial relaxation timescale, which becomes $\sim$ 2 times faster just below T_C (Fig. 3c) and below the critical fluence, f_{sat}^{SC} [22], i.e., when the superconducting state is non-thermally quenched [18]. Since the non-thermal quenching of the superconducting phase is driven on a timescale faster than the lattice heating, this result demonstrates that the observed changes in the PG dynamics are a genuine result of the interplay between the PG and SC phases without any role played by the lattice temperature.

In summary the main changes to the PG component dynamics that sharply occur once the SC phase sets in are: i) the perturbation decreases by about a factor of two at constant pump fluence (10 μJ/cm^2), ii) the initial relaxation dynamics proceed about 2 times faster, iii) a slightly negative variation is observed after about 0.5 ps.

These results can be consistently interpreted within a two-component time-dependent GL model, under the assumption that the pseudogap has a broken symmetry [5, 28, 29]. In facts an increasing number of experiments suggest the presence of an order parameter in the pseudogap phase, i.e., below T* [30, 31]. Remarkably the onset temperature of the PG component measured in this work (Fig. 3b) exactly coincides with the T* reported on similar samples [31]. The nature of this order parameter is still under debate, and the discussion will be kept at the most general level, considering the only assumption that ψ_{SC} and ψ_{PG} are two complex order parameters that break different symmetries. In this case the lowest-order symmetry-allowed GL functional is [8, 29]:

$$F = \alpha_{SC}|\psi_{SC}|^2 + \beta_{SC}|\psi_{SC}|^4 + \alpha_{PG}|\psi_{PG}|^2 + \\ +\beta_{PG}|\psi_{PG}|^4 + W|\psi_{SC}|^2|\psi_{PG}|^2 \quad (2)$$

where the GL expansion is up to quartic order, with α_k and β_k as expansion coefficients, and the interaction term couples the squares of the order parameters, with sign and strength determined by W. The kinetic equation for each order parameter can be obtained through the relation $d\psi/dt = -\gamma\partial F/\partial\psi^*$, where γ is a constant kinetic coefficient [32]. Following Refs. 33 this expression can be linearized for small perturbations of the PG and SC order parameter amplitudes, yielding a set of differential equations of the same form as Eq. 1 which reproduce the data reported in this Letter [22].

This simple model is not comprehensive [33, 34], but it captures the main physics of the coupling between the two relaxation dynamics. The mixed term contains some crucial information, as its sign directly derives from W. A positive mixed term implies a repulsive coupling W, and in turn a competition between order parameters. Fig.4 shows the non-equilibrium PG phase dynamics predicted by the time-dependent GL model for three different couplings W. The results reported here clearly correspond to the repulsive, $W > 0$, case.

To obtain a quantitative estimate of the strength of the coupling it is possible to calculate the dimensionless ratio

$$\frac{\tau_{21}}{\tau_{22}} = \frac{W}{\sqrt{2\beta_{SC}\beta_{PG}}}\frac{\sqrt{\alpha_{SC}\alpha_{PG} - \mathcal{O}(W)}}{-\alpha_{SC} - \mathcal{O}(W)} \quad (3)$$

where the terms of higher order, $\mathcal{O}(W)$, can be neglected for small W. By considering the experimental values of τ_{22} and τ_{21} and by using the parametrization reported in [9], it is possible to estimate the ratio $W/\sqrt{\beta_{SC}\beta_{PG}} \sim 10^{-2}$. A ratio smaller than 1 indicates that phase competition is weak enough to allow the coexistence of PG and SC phases [8], therefore rationalizing the apparent dichotomy of coexistence and competition reported in the literature [10, 12, 15].

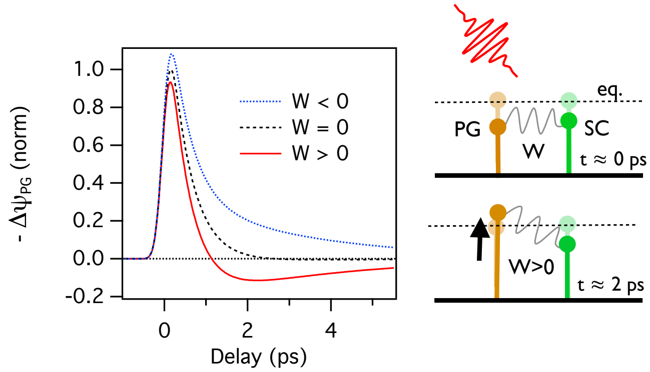

FIG. 4. Dynamics of the PG order parameter obtained from the time-dependent GL model (see text) for the case of three different couplings, repulsive ($W > 0$), attractive ($W < 0$) and no interaction ($W = 0$). The repulsive ($W < 0$) case better reproduces the experimental data (Fig.2 and 3). A schematic representation of the order parameter dynamics after photoexcitation is shown on the right side. The height of the brown (green) symbols indicates the amplitude of the PG (SC) order parameters. Due to the different relaxation timescales, after $\sim$ 2 ps (lower panel) only the PG order parameter is close to the equilibrium value and exhibits a small enhancement due to the repulsive interaction with the SC order parameter.

In conclusion, ultrafast broadband transient reflectivity experiments allow to identify and measure the dynamics of PG and SC phases in underdoped $Bi_2Sr_2Ca_{0.92}Y_{0.08}Cu_2O_{8+\delta}$ single crystals (T_c = 85 K), by disentangling their spectro-temporal signatures in the out-of-equilibrium reflectivity data. The results prove the existence of a coupled dynamics for the PG and for the SC order parameter. The data, interpreted within a time-dependent GL approach under the assumption that the PG phase has a broken symmetry, suggest a weak positive interaction between the order parameters, leading to the coexistence of the two competing phases. The ability to quantitatively estimate these coupling parameters paves the way for further applications of ultrafast broadband reflectivity to a variety of complex systems characterized by interacting, yet coexisting, phases [2–4, 6, 7].

We acknowledge discussions and suggestions from M. Schirò, M. Capone and A. Avella. F.C., G.C., and F.P. acknowledge the support of the Italian Ministry of University and Research under Grant Nos. FIRBR-BAP045JF2 and FIRB-RBAP06AWK3. The research activities of C.G., S.D.C. and F.P. have received funding from the European Union, Seventh Framework Programme (FP7 2007-2013), under grant agreement nr. 280555. The crystal growth work was performed in M.G.s prior laboratory at Stanford University, Stanford, CA 94305, USA, and supported by DOE under Contract No. DE-AC03-76SF00515. The work at UBC was supported by the Alfred P. Sloan Foundation (A.D.), the CRC, Killam, and NSERC's Steacie Fellowship Programs (A.D.), NSERC, CFI, CIFAR Quantum Materials, and BCSI.

---

* Present Address: Materials Sciences Division, Lawrence Berkeley National Laboratory, Berkeley, CA 94720, USA

† Present Address: European XFEL Facility, Hamburg 22607, Germany

‡ Present Address: Radboud University Nijmegen, Nijmegen, 6525 AJ, Netherlands

[1] M. Norman, D. Pines, and C. Kallin, Adv. Phys., **54**, 715 (2005).
[2] G. Stewart, Rev. Mod. Phys., **83**, 1589 (2011).
[3] Y. Tokura, Rep. Prog. Phys., **69**, 797 (2006).
[4] J. Mydosh and P. Oppeneer, Rev. Mod. Phys., **83**, 1301 (2011).
[5] S. Sachdev, Science, **288**, 475 (2000).
[6] E. Dagotto, T. Hotta, and A. Moreo, Physics Reports, **344**, 1 (2001).
[7] S. Maiti and A. Chubukov, Phys. Rev. B, **82** 214515 (2010).
[8] J.-H. She, J. Zaanen, A. Bishop, and A. Balatsky, Phys. Rev. B, **82**, 165128 (2010).
[9] S. Chakravarty, H.-Y. Kee, and K. Völker, Nature, **428**, 53 (2004).
[10] R. Khasanov, T. Kondo, S. Strässle, D. Heron, A. Kaminski, H. Keller, S. Lee, and T. Takeuchi, Phys. Rev. Lett., **101**, 227002 (2008); T. Kondo, R. Khasanov, T. Takeuchi, J.Schmalian, and A. Kaminski, Nature, **457**, 296 (2009).
[11] V. J. Emery and S. A. Kivelson, Nature, **374**, 434 (1995).
[12] A. Kanigel, U. Chatterjee, M. Randeria, M. Norman, G. Koren, K. Kadowaki, and J. Campuzano, Phys. Rev. Lett., **101**, 137002 (2008); H.-B. Yang, J. D. Rameau, P. D. Johnson, T. Valla, A. Tsvelik, and G. D. Gu, Nature, **456**, 77 (2008); Y. Kohsaka, T. Hanaguri, M. Azuma, M. Takano, J. C. Davis, and H. Takagi, Nat. Phys., **8**, 534 (2012).
[13] A. Damascelli, Z. Hussain, and Z.-X. Shen, Rev. Mod. Phys., **75**, 473 (2003); W. S. Lee, I. M. Vishik, K. Tanaka, D. H. Lu, T. Sasagawa, N. Nagaosa, T. P. Devereaux, Z. Hussain, and Z.-X. Shen, Nature, **450**, 81 (2007).
[14] A. Pushp, C. V. Parker, A. N. Pasupathy, K. K. Gomes, S. Ono, J. Wen, Z. Xu, G. Gu, and A. Yazdani, Science, **324**, 1689 (2009); J. W. Alldredge *et al.*, Nat. Phys., **4**, 319 (2008).
[15] E. Chia, J.-X. Zhu, D. Talbayev, R. Averitt, A. Taylor, K.-H. Oh, I.-S. Jo, and S.-I. Lee, Phys. Rev. Lett., **99**, 147008 (2007); J. P. Hinton, J. D. Koralek, G. Yu, E. M. Motoyama, Y. M. Lu, A. Vishwanath, M. Greven, and J. Orenstein, arXiv:1208.0960.
[16] Y. H. Liu *et al.*, Phys. Rev. Lett., **101**, 137003 (2008); Y. Toda, T. Mertelj, P. Kusar, T. Kurosawa, M. Oda, M. Ido, and D. Mihailovic, Phys. Rev. B, **84**, 174516 (2011).
[17] The *local equilibrium approximation* holds when $(Dk^2, \omega) \ll \gamma$, where D is the diffusion coefficient, k and ω are the typical wavenumber and frequencies of QP and γ is the inelastic damping rate of the electron system [19]. By considering known optical data [24] and that photoexcitations at 1.5 eV rapidly relax to the energy of the corresponding gap one can easily verify the validity of this assumption. The connection between excitations dynamics and order parameter dynamics is also supported by comparing our results to direct measurements of the condensate dynamics at THz frequencies [35].
[18] P. Kusar, V. Kabanov, J. Demsar, T. Mertelj, S. Sugai, and D. Mihailovic, Phys. Rev. Lett., **101**, 227001 (2008); C. Giannetti, G. Coslovich, F. Cilento, G. Ferrini, H. Eisaki, N. Kaneko, M. Greven, and F. Parmigiani, Phys. Rev. B, **79**, 224502 (2009); G. Coslovich *et al.*, *ibid.*, **83**, 064519 (2011).
[19] A. M. Gulian and G. F. Zharkov, *Nonequilibrium Electrons and Phonons in Superconductors* (Kluwer Academic/Plenum Publishers, New York, 1999).
[20] M. Eckstein, M. Kollar, and P. Werner, Phys. Rev. Lett., **103**, 056403 (2009); M. Schiró, Phys. Rev. B, **81**, 085126 (2010); A. Schnyder, D. Manske, and A. Avella, *ibid.*, **84**, 214513 (2011).
[21] F. Cilento, C. Giannetti, G. Ferrini, S. D. Conte, T. Sala, G. Coslovich, M. Rini, A. Cavalleri, and F. Parmigiani, Appl. Phys. Lett., **96**, 021102 (2010).
[22] See Supplemental Material at [URL] for further details.
[23] H. Eisaki, N. Kaneko, D. L. Feng, A. Damascelli, P. K. Mang, K. M. Shen, Z. Shen, and M. Greven, Phys. Rev. B, **69**, 064512 (2004).
[24] C. Giannetti *et al.*, Nat. Commun., **2**, 353 (2011).
[25] O. Alter, P. O. Brown, and D. Botstein, Proc. Natl. Acad. Sci., **97**, 10101 (2000); E. R. Henry, Biophys. J., **72**, 652 (1997).
[26] R. Kaindl, M. Woerner, T. Elsaesser, D. C. S. J. Ryan, G. Farnan, M. McCurry, and D. Walmsley, Science, **287**, 470 (2000).
[27] S. Dal Conte *et al.*, Science **335**, 1600 (2012).
[28] C. Varma, Phys. Rev. Lett., **83**, 3538 (1999).
[29] S. Chakravarty, R. Laughlin, D. Morr, and C. Nayak, Phys. Rev. B, **63**, 094503 (2001).
[30] B. Fauqué, Y. Sidis, V. Hinkov, S. Pailhès, C. T. Lin, X. Chaud, and P. Bourges, Phys. Rev. Lett., **96**, 197001 (2006); Y. Li, V. Balédent, N. Barišić, Y. Cho, B. Fauqué, Y. Sidis, G. Yu, X. Zhao, P. Bourges, and M. Greven, Nature, **455**, 372 (2008); R.-H. He *et al.*, Science, **331**, 1579 (2011).
[31] S. De Almeida-Didry, Y. Sidis, V. Balédent, F. Giovannelli, I. Monot-Laffez, and P. Bourges, Phys. Rev. B, **86**, 020504 (2012).
[32] E. M. Lifshitz and L. P. Pitaevskii, *Physical Kinetics* (Butterworth-Heinemann, Oxford, 1981).
[33] P. Konsin and T. Örd, Physica C, **191**, 469 (1992); P. Konsin and B. Sorkin, JPCS, **150**, 052122 (2009).
[34] P. Kusar, I. Madan, M. Lu-Dac, T. Mertelj, V. V. Kabanov, S. Sugai, and D. Mihailovic, arXiv:1207.2879.
[35] R. Averitt, G. Rodriguez, A. Lobad, J. Siders, S. Trugman, and A. Taylor, Phys. Rev. B, **63**, 140502 (2001);

M. Beyer, D. Städter, M. Beck, H. Schäfer, V. Kabanov, G. Logvenov, I. Bozovic, G. Koren, and J. Demsar, *ibid.*, **83**, 214515 (2011).